

Critical parameters of consistent relativistic mean-field models

O. Lourenço¹, M. Dutra², and D. P. Menezes³

¹*Universidade Federal do Rio de Janeiro, 27930-560, Macaé, RJ, Brazil*

²*Departamento de Ciências da Natureza - IHS, Universidade Federal Fluminense, 28895-532 Rio das Ostras, RJ, Brazil*

³*Depto de Física - CFM - Universidade Federal de Santa Catarina, Florianópolis - SC - CP. 476 - CEP 88.040 - 900 - Brazil*

(Dated: September 28, 2018)

In the present work, the critical temperature, critical pressure and critical density, known as the critical parameters related to the liquid-gas phase transition are calculated for 34 relativistic mean-field models, which were shown to satisfy nuclear matter constraints in a comprehensive study involving 263 models. The compressibility factor was calculated and all 34 models present values lower than the one obtained with the van der Waals equation of state. The critical temperatures were compared with experimental data and just two classes of models can reach values close to them. A correlation between the critical parameters and the incompressibility was obtained.

PACS numbers: 21.30.Fe, 21.65.Cd, 26.60.Kp, 24.10.Jv

I. INTRODUCTION

The understanding of nuclear matter properties is of fundamental importance as a guide towards more specific subjects, such as nuclear and hadron spectroscopy, heavy-ion collisions, caloric curves and negative heat capacities, nuclear multifragmentation and distillation effects, neutron stars and the possible existence of the pasta phase in its core and even the QCD phase diagram and its phase transitions. At low densities and relatively low temperatures (below 20 MeV), nuclear matter can evolve through different phase separation boundaries and the construction of binodals depicts very well this problem. Another important aspect is the investigation of instability boundaries and the spinodals are used to separate unstable from stable matter. These sections (binodals and spinodals) are just a reflex of the well known fact that at low densities, nuclear matter undergoes a first order phase transition, which belongs to the liquid-gas universality class [1–3].

A seminal work on the use of relativistic models to describe multicomponent systems (in nuclear matter, the components are protons and neutrons) is [2]. This extremely didactic paper clearly shows how the geometrical Maxwell construction can be used to determine the amount of particles (proton fraction) and the related chemical potentials in the coexistence phase and the construction of the binodal section. As far as unstable matter is concerned, the instabilities a system may present are related to the possible phase transitions it can undertake [3]. Spinodal sections are obtained from the derivative of the free energy of the system with respect to the chemical potentials of its components. The spinodal instability is known to lead to a liquid-gas phase transition with the restoration of the isospin symmetry at a certain density.

In Ref. [2], a three dimensional plot (see Fig. 7) shows the phase coexistence boundary in a pressure-temperature-proton fraction plane, from where it is seen that the critical temperature always takes place in the

symmetric matter. Analogously, in [5], it was shown that the instability region decreases with the increase of the temperature up to a certain *critical temperature*, which is related to a *critical pressure* and *critical density*. For temperatures larger than the critical temperature, the system is stable. Once again, these *critical parameters* always take place at proton fraction 0.5, i.e., symmetric nuclear matter (see Table IV).

Nevertheless, the values of these critical parameters are model dependent and there are many nonrelativistic [4] and relativistic models [5] in the market, which can be used to calculate binodals and spinodals. The references just given show only a few of them. In the present work we restrict our investigation to specific relativistic mean-field (RMF) models, which were shown to satisfy important nuclear matter bulk properties in Ref. [6]. They are named here as consistent relativistic mean field parametrizations (CRMF) and in the next section a more detailed explanation on this choice is made.

After the presentation of 34 CRMF models, we show how the critical parameters are obtained and their values are displayed and compared with experimental results. The conclusions are drawn in the last section of the present work.

II. CONSISTENT RELATIVISTIC MEAN-FIELD MODELS

The analysis performed in Ref. [6] pointed out to only 35 parametrizations, out of 263 investigated, simultaneously approved in seven distinct nuclear matter constraints. These consistent RMF parametrizations had their bulk and thermodynamical quantities compared to respective theoretical/experimental data from symmetric nuclear matter (SNM), pure neutron matter (PNM) and a mixture of both, namely, symmetry energy and its slope evaluated at the saturation density ρ_0 , and the ratio of the symmetry energy at $\rho_0/2$ to its value at ρ_0 (MIX). These detailed constraints are specified in Table I.

In Ref. [6], the models were divided into seven different categories and only three of these categories included models that satisfies the imposed constraints. Among the 35 CRMF parametrizations, 30 of them are of type 4 [6], i.e., the Lagrangian density comprises non-linear σ and ω terms and cross terms involving these fields. They are: BKA20 [7], BKA22 [7], BKA24 [7], BSR8 [8], BSR9 [8], BSR10 [8], BSR11 [8], BSR12 [8], BSR15 [8], BSR16 [8], BSR17 [8], BSR18 [8], BSR19 [8], BSR20 [8], FSU-III [9], FSU-IV [9], FSUGold [10], FSUGold4 [11], FSUGZ03 [12], FSUGZ06 [12], G2* [13], IU-FSU [14], Z271s2 [15], Z271s3 [15], Z271s4 [15], Z271s5 [15], Z271s6 [15], Z271v4 [15], Z271v5 [15], and Z271v6 [15]. The Lagrangian density that describes such parametrizations is

$$\begin{aligned} \mathcal{L}_{\text{NL}} = & \bar{\psi}(i\gamma^\mu\partial_\mu - M)\psi + g_\sigma\sigma\bar{\psi}\psi - g_\omega\bar{\psi}\gamma^\mu\omega_\mu\psi \\ & - \frac{g_\rho}{2}\bar{\psi}\gamma^\mu\vec{\rho}_\mu\vec{\tau}\psi + \frac{1}{2}(\partial^\mu\sigma\partial_\mu\sigma - m_\sigma^2\sigma^2) - \frac{A}{3}\sigma^3 \\ & - \frac{B}{4}\sigma^4 - \frac{1}{4}F^{\mu\nu}F_{\mu\nu} + \frac{1}{2}m_\omega^2\omega_\mu\omega^\mu + \frac{C}{4}(g_\omega^2\omega_\mu\omega^\mu)^2 \\ & - \frac{1}{4}\vec{B}^{\mu\nu}\vec{B}_{\mu\nu} + \frac{1}{2}m_\rho^2\vec{\rho}_\mu\vec{\rho}^\mu + \frac{1}{2}\alpha'_3g_\omega^2g_\rho^2\omega_\mu\omega^\mu\vec{\rho}_\mu\vec{\rho}^\mu \\ & + g_\sigma g_\omega^2\sigma\omega_\mu\omega^\mu \left(\alpha_1 + \frac{1}{2}\alpha'_1g_\sigma\sigma \right) \\ & + g_\sigma g_\rho^2\sigma\vec{\rho}_\mu\vec{\rho}^\mu \left(\alpha_2 + \frac{1}{2}\alpha'_2g_\sigma\sigma \right), \end{aligned} \quad (1)$$

with $F_{\mu\nu} = \partial_\nu\omega_\mu - \partial_\mu\omega_\nu$ and $\vec{B}_{\mu\nu} = \partial_\nu\vec{\rho}_\mu - \partial_\mu\vec{\rho}_\nu$. The nucleon mass is M and the meson masses are m_j , for $j = \sigma, \omega$, and ρ .

The other 4 CRMF approved parametrizations present density dependent (DD) coupling constants. Two of them are standard DD parametrizations: DD-F [16] and TW99 [17], and the remaining two also present the δ meson in their structures: DDH δ [18] and DD-ME δ [19]. The Lagrangian density of all of them is expressed as,

$$\begin{aligned} \mathcal{L}_{\text{DD}} = & \bar{\psi}(i\gamma^\mu\partial_\mu - M)\psi + \Gamma_\sigma(\rho)\sigma\bar{\psi}\psi - \Gamma_\omega(\rho)\bar{\psi}\gamma^\mu\omega_\mu\psi \\ & - \frac{\Gamma_\rho(\rho)}{2}\bar{\psi}\gamma^\mu\vec{\rho}_\mu\vec{\tau}\psi + \Gamma_\delta(\rho)\bar{\psi}\vec{\delta}\vec{\tau}\psi - \frac{1}{4}F^{\mu\nu}F_{\mu\nu} \\ & + \frac{1}{2}(\partial^\mu\sigma\partial_\mu\sigma - m_\sigma^2\sigma^2) + \frac{1}{2}m_\omega^2\omega_\mu\omega^\mu - \frac{1}{4}\vec{B}^{\mu\nu}\vec{B}_{\mu\nu} \\ & + \frac{1}{2}m_\rho^2\vec{\rho}_\mu\vec{\rho}^\mu + \frac{1}{2}(\partial^\mu\vec{\delta}\partial_\mu\vec{\delta} - m_\delta^2\vec{\delta}^2), \end{aligned} \quad (2)$$

TABLE I. Set of updated constraints (SET2a) used in Ref. [6]. See that reference for more details concerning each constraint.

Constraint	Quantity	Density Region	Range of constraint
SM1	K_0	at ρ_0	190 – 270 MeV
SM3a	$P(\rho)$	$2 < \frac{\rho}{\rho_0} < 5$	Band Region
SM4	$P(\rho)$	$1.2 < \frac{\rho}{\rho_0} < 2.2$	Band Region
PNM1	$\mathcal{E}_{\text{PNM}/\rho}$	$0.017 < \frac{\rho}{\rho_0} < 0.108$	Band Region
MIX1a	J	at ρ_0	25 – 35 MeV
MIX2a	L_0	at ρ_0	25 – 115 MeV
MIX4	$\frac{S(\rho_0/2)}{J}$	at ρ_0 and $\rho_0/2$	0.57 – 0.86

where

$$\Gamma_i(\rho) = \Gamma_i(\rho_0)f_i(x); \quad f_i(x) = a_i \frac{1 + b_i(x + d_i)^2}{1 + c_i(x + d_i)^2}, \quad (3)$$

for $i = \sigma, \omega$, and $x = \rho/\rho_0$. The Lagrangian density describing the DD-F and TW99 [17] parametrizations is the same as the one in Eq. (2) when the meson δ is not taken into account.

The last CRMF parametrization is a point-coupling model [20–26]: FA3 [27]. Here, we do not investigate such model since in a previous work [28] we have showed it is not capable of generating, already in the zero temperature regime, a mass radius curve for neutron stars, due to a very particular behavior in the high-density regime, namely, a fall in the pressure versus energy density (ε) curve near $\varepsilon = 4.1 \text{ fm}^{-4}$. For that reason, we have decided to discard this particular parametrization from our finite temperature analysis.

III. RESULTS FROM FINITE TEMPERATURE REGIME

We next present only the main formulae for the calculation of the critical parameters. All other calculations and the complete equations of state are given in detail in Ref. [6] and we do reproduce them here.

A. Critical parameters, and model dependence in the liquid phase

The CRMF critical parameters are obtained directly from the thermodynamical pressure (P) of these models once the following conditions in the $P \times \rho$ plane are imposed:

$$P_c = P(\rho_c, T_c), \quad \left. \frac{\partial P}{\partial \rho} \right|_{\rho_c, T_c} = 0, \quad \left. \frac{\partial^2 P}{\partial \rho^2} \right|_{\rho_c, T_c} = 0, \quad (4)$$

where P_c , ρ_c and T_c are, respectively, the critical pressure, density and temperature. These three critical parameters define a unique critical point. Such constraints can be used because hadronic mean-field models present the same features exhibited by the van der Waals model, i. e., a liquid gas phase transition at temperatures smaller than T_c , see Refs. [2, 29–36], for instance.

From the Lagrangian density in Eq. (1), one can derive the expression for symmetric nuclear matter ($\gamma = 4$) pressure, by following, for example, the steps indicating in Ref. [37]. The result is

$$\begin{aligned} P_{\text{NL}} = & -\frac{1}{2}m_\sigma^2\sigma^2 - \frac{A}{3}\sigma^3 - \frac{B}{4}\sigma^4 + \frac{1}{2}m_\omega^2\omega_0^2 + \frac{C}{4}(g_\omega^2\omega_0^2)^2 \\ & + g_\sigma g_\omega^2\sigma\omega_0^2 \left(\alpha_1 + \frac{1}{2}\alpha'_1g_\sigma\sigma \right) \\ & + \frac{\gamma}{6\pi^2} \int_0^\infty \frac{dk k^4}{(k^2 + M^{*2})^{1/2}} [n(k, T, \mu^*) + \bar{n}(k, T, \mu^*)], \end{aligned} \quad (5)$$

where

$$n(k, T, \mu^*) = \frac{1}{e^{(E^* - \mu^*)/T} + 1}, \quad \text{and} \\ \bar{n}(k, T, \mu^*) = \frac{1}{e^{(E^* + \mu^*)/T} + 1} \quad (6)$$

are the Fermi-Dirac distributions for particles and antiparticles, respectively. The effective energy, nucleon mass, and chemical potential are $E^* = (k^2 + M^{*2})^{1/2}$, $M^* = M - g_\sigma \sigma$, and $\mu^* = \mu - g_\omega \omega_0$, respectively. Furthermore, the (classical) mean-field values of σ and ω_0 are found by solving the following system of equations,

$$m_\sigma^2 \sigma = g_\sigma \rho_s - A\sigma^2 - B\sigma^3 + g_\sigma g_\omega^2 \omega_0^2 (\alpha_1 + \alpha'_1 g_\sigma \sigma) \quad (7) \\ m_\omega^2 \omega_0 = g_\omega \rho - C g_\omega (g_\omega \omega_0)^3 - g_\sigma g_\omega^2 \sigma \omega_0 (2\alpha_1 + \alpha'_1 g_\sigma \sigma), \quad (8)$$

with

$$\rho = \frac{\gamma}{2\pi^2} \int_0^\infty dk k^2 [n(k, T, \mu^*) - \bar{n}(k, T, \mu^*)], \quad (9) \\ \rho_s = \frac{\gamma}{2\pi^2} \int_0^\infty \frac{dk M^* k^2}{(k^2 + M^{*2})^{1/2}} [n(k, T, \mu^*) + \bar{n}(k, T, \mu^*)]. \quad (10)$$

It is worth noticing in these derivations that $\langle \vec{\rho}_\mu \rangle \equiv \bar{\rho}_{0(3)}$, and $\langle \vec{\delta} \rangle \equiv \delta_{(3)}$ are vanishing, since we are restricted to the symmetric nuclear matter system, in which $\rho_p = \rho_n$ and $\rho_{sp} = \rho_{sn}$. For that reason, terms in Eq. (1) involving specifically these fields do not contribute to the thermodynamical quantities of the model, or in any other calculations in the mean-field approximation.

The same procedures exposed in Ref. [37] are also used in order to generate the pressure for the density dependent model described by Eq. (2). Once again, the fields $\bar{\rho}_{0(3)}$ and $\delta_{(3)}$ do not contribute for the calculations. Therefore, the thermodynamics of DD-F and TW99 parametrizations is exactly the same of the DDH δ and DD-ME δ ones. In particular, the symmetric nuclear matter pressure reads

$$P_{\text{DD}} = \rho \Sigma_R(\rho) - \frac{1}{2} m_\sigma^2 \sigma^2 + \frac{1}{2} m_\omega^2 \omega_0^2 \\ + \frac{\gamma}{6\pi^2} \int_0^\infty \frac{dk k^4}{(k^2 + M^{*2})^{1/2}} [n(k, T, \mu^*) + \bar{n}(k, T, \mu^*)], \quad (11)$$

with the rearrangement term defined as

$$\Sigma_R(\rho) = \frac{\partial \Gamma_\omega}{\partial \rho} \omega_0 \rho - \frac{\partial \Gamma_\sigma}{\partial \rho} \sigma \rho_s. \quad (12)$$

The mean-fields σ and ω_0 are given by

$$\sigma = \frac{\Gamma_\sigma(\rho)}{m_\sigma^2} \rho_s, \quad \text{and} \quad \omega_0 = \frac{\Gamma_\omega(\rho)}{m_\omega^2} \rho, \quad (13)$$

with the functional forms of ρ and ρ_s given as in the nonlinear model, Eqs. (9)-(10), with the same distributions

functions of Eq. (6), and the same form for the effective energy E^* . The effective nucleon mass and chemical potential are now given, respectively, by $M^* = M - \Gamma_\sigma(\rho)\sigma$, and $\mu^* = \mu - \Gamma_\omega(\rho)\omega_0 - \Sigma_R(\rho)$.

Since the expressions given in Eqs. (5) and (11) are completely determined, we are able to apply the conditions to calculate the critical point given in Eq. (4) and then obtain P_c , ρ_c and T_c for each of the CRMF parametrizations. These results are presented in Table II. Also in this Table, we furnish the compressibility factor, defined as $Z_c = P_c / \rho_c T_c$. For the van der Waals (vdW) equation of state (EOS), for example, this quantity has a value of 0.375, independently of the fluid described by it. This is a direct consequence of the universality of the vdW EOS. We have divided the 34 CRMF models into 6 families. Notice that all CRMF parametrizations present $Z_c < 0.375$.

TABLE II. Critical parameters (T_c , ρ_c and P_c), and compressibility factor ($Z_c = P_c / \rho_c T_c$) of CRMF parametrizations.

Model	T_c (MeV)	ρ_c (fm $^{-3}$)	P_c (MeV/fm 3)	$\frac{P_c}{\rho_c}$	Z_c
BKA20	14.92	0.0458	0.209	0.314	0.306
BKA22	13.91	0.0442	0.178	0.300	0.290
BKA24	13.83	0.0450	0.177	0.306	0.284
BSR8	14.17	0.0440	0.185	0.300	0.297
BSR9	14.11	0.0450	0.185	0.305	0.291
BSR10	13.90	0.0439	0.176	0.297	0.288
BSR11	14.00	0.0442	0.179	0.301	0.289
BSR12	14.15	0.0448	0.185	0.304	0.292
BSR15	14.53	0.0456	0.199	0.313	0.300
BSR16	14.44	0.0454	0.196	0.311	0.299
BSR17	14.32	0.0451	0.191	0.308	0.296
BSR18	14.25	0.0451	0.189	0.309	0.294
BSR19	14.28	0.0451	0.190	0.308	0.295
BSR20	14.41	0.0464	0.197	0.318	0.295
FSU-III	14.75	0.0461	0.205	0.311	0.301
FSU-IV	14.75	0.0461	0.205	0.311	0.301
FSUGold	14.75	0.0461	0.205	0.311	0.301
FSUGold4	14.80	0.0456	0.204	0.309	0.302
FSUGZ03	14.11	0.0450	0.185	0.305	0.291
FSUGZ06	14.44	0.0454	0.196	0.311	0.299
IU-FSU	14.49	0.0457	0.196	0.295	0.296
G2*	14.38	0.0468	0.192	0.305	0.285
Z271s2	17.97	0.0509	0.303	0.343	0.331
Z271s3	17.97	0.0509	0.303	0.343	0.331
Z271s4	17.97	0.0509	0.303	0.343	0.331
Z271s5	17.97	0.0509	0.303	0.343	0.331
Z271s6	17.97	0.0509	0.303	0.343	0.331
Z271v4	17.97	0.0509	0.303	0.343	0.331
Z271v5	17.97	0.0509	0.303	0.343	0.331
Z271v6	17.97	0.0509	0.303	0.343	0.331
DD-F	15.24	0.0505	0.245	0.343	0.318
TW99	15.17	0.0509	0.241	0.332	0.312
DDH δ	15.17	0.0509	0.241	0.332	0.312
DD-ME δ	15.32	0.0491	0.235	0.323	0.312

In Fig. 1, we present the density dependence of the pressure for the CRMF parameterizations, in units of P_c and ρ_c , all of them at $T = T_c$. In this figure, we notice an interesting feature also reported for the Boguta-Bodmer models analyzed in Ref. [32] (see Fig. 1 of this reference), namely, the scaled curves are indistinguishable in the gaseous phase ($\rho/\rho_c < 1$) and distinct from each other, i.e., model dependent, in the liquid phase region ($\rho/\rho_c > 1$). The authors of Ref. [32] claimed that in the latter region, the nucleons are confined to a smaller phase space, approaching each other progressively and al-

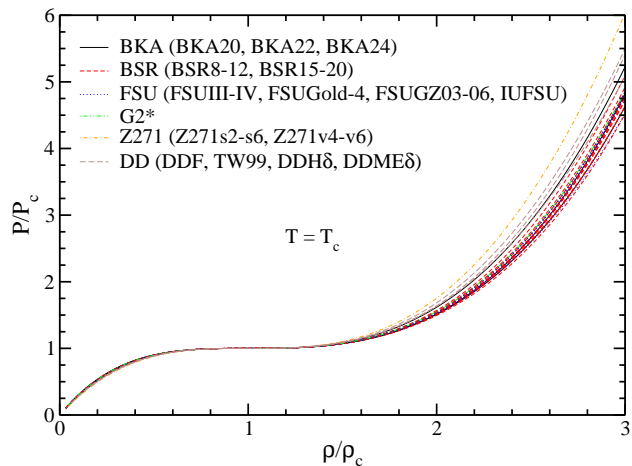


FIG. 1. Pressure as a function of density, both in units of their respective critical values, for the CRMF parametrizations at $T = T_c$.

lowing the interactions to take place more substantially. This phenomenology is reflected by the scaling, exhibited for $\rho/\rho_c < 1$, and absent in the remaining region. As the structure of the parametrizations analyzed in Ref. [32] was restricted to RMF models presenting only third- and fourth order self-interactions in the scalar field σ (Boguta-Bodmer model), it was difficult to generalize such result to any RMF parametrization. However, here we investigate more sophisticated RMF models, including that one where the couplings are density dependent, and the phenomenology of the liquid phase presented in the Boguta-Bodmer model was showed again, indicating the general trend of RMF parametrizations of any kind in presenting a model dependence in the liquid phase, and a scaling in the gaseous one, at symmetric nuclear matter environment.

B. Comparison with experimental data

As a further analysis of the CRMF critical parameters, we compared such quantities with known experimental data. Firstly, we compare the critical temperature in Fig. 2.

We can see that only a few parametrizations reach some of experimental points. The density dependent TW99, DD-F, DDH δ and DD-ME δ [19] present T_c inside the range of $15 \leq T_c \leq 19$ MeV [41], and the family Z271, that encompasses all 8 related parametrizations, has the critical temperature compatible with 5 of the 8 experimental points, including the more recent one of Ref. [44].

In this latter work [44], the authors were able to experimentally determine all three critical parameters, unlike previous studies focusing only in T_c . For that purpose, they have used two types of experiments, namely, compound-nucleus and nuclear multifragmentation. In the former, two different nuclei collide

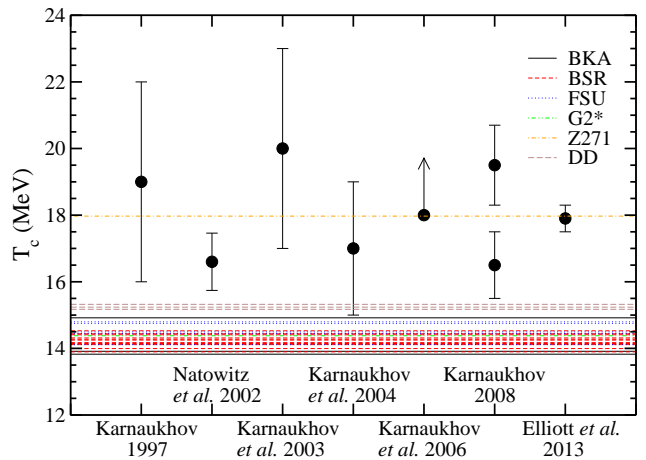


FIG. 2. Critical temperature of CRMF parametrizations compared with experimental data (circles) collected from the following references: Karnaukhov 1997 [38], Natowitz *et al.* 2002 [39], Karnaukhov *et al.* 2003 [40], Karnaukhov *et al.* 2004 [41], Karnaukhov *et al.* 2006 [42], Karnaukhov 2008 [43], and Elliott *et al.* 2013 [44]. The parametrization families are indicated as in Fig. 1.

with each other and form a single compound system, with excitation energy obtained from the energy and masses of the subsystems. They have analyzed results from the following compound-nucleus reactions: $^{58}\text{Ni} + ^{12}\text{C} \rightarrow ^{70}\text{Se}$ and $^{64}\text{Ni} + ^{12}\text{C} \rightarrow ^{76}\text{Se}$, performed at the 88-in. cyclotron of the Lawrence Berkeley National Laboratory (LBNL) [45]. In the latter experiment in that study, a beam of relativistic incident light particles was used to heat a particular target nucleus. The intermediate-mass fragments emitted in this multifragmentation process are essential for determination of thermal quantities. In Ref. [44], the authors also studied the multifragmentation reactions, performed by the Indiana Silicon Sphere Collaboration at the Alternating Gradient Synchrotron at Brookhaven National Laboratory [46], and by the Equation of State Collaboration at LBNL. The studied reactions were 1 GeV/c $\pi + ^{197}\text{Au}$, 1 GeV/nucleon $^{197}\text{Au} + ^{12}\text{C}$, 1 GeV/nucleon $^{139}\text{La} + ^{12}\text{C}$, and 1 GeV/nucleon $^{84}\text{Kr} + ^{12}\text{C}$. The yields of all these reactions were analyzed within a Fisher droplet model, modified to take into account asymmetry, Coulomb and finite-size effects, and angular momentum arising from the collisions. The analyzed results from all these compound-nucleus and multifragmentation reactions, pointed out to $T_c = 17.9 \pm 0.4$ MeV, $P_c = 0.31 \pm 0.07$ MeV/fm 3 , and $\rho_c = 0.06 \pm 0.01$ fm $^{-3}$, for the critical parameters of symmetric nuclear matter.

As mentioned before, the family of parametrizations named as Z271 has exactly the same experimental value of T_c from Ref. [44], as we can see in Fig. 2. For the sake of completeness concerning P_c and ρ_c , we have also compared these particular critical values of the CRMF parametrizations to those experimental ones of Ref. [44], namely, $P_c = 0.31 \pm 0.07$ MeV/fm 3 , and $\rho_c = 0.06 \pm$

0.01 fm^{-3} . The results are depicted in Fig. 3. As we can see, once more the set of Z271 parametrizations completely agrees with the data. Specifically for these critical parameters, we also notice agreement of the density dependent model with the experiments. The remaining CRMF parametrizations are not inside the boundaries.

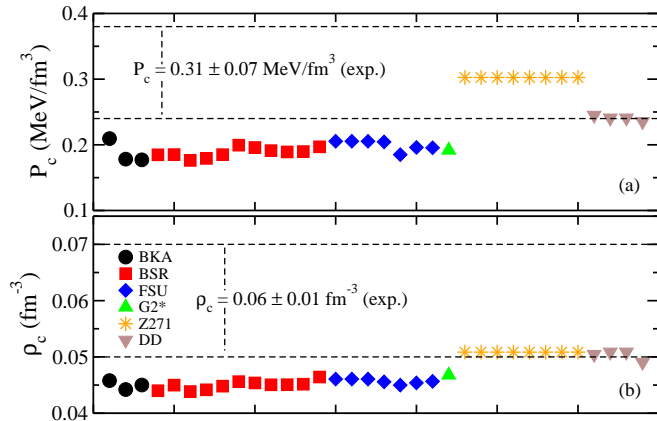


FIG. 3. Critical (a) pressure and (b) density for all CRMF parametrizations, compared with the corresponding experimental values extracted from Ref. [44].

By analyzing in detail the Z271 family [15], we observe that in all eight parametrizations the couplings α_1 and α'_1 are vanishing, and $C \neq 0$ is the only constant that differs these parametrizations from those of the Boguta-Bodmer model, see Eq. (5). There are no interactions between mesons in this case for symmetric nuclear matter, only self-interactions. In some sense, the density dependent model has a similar structure, since the nonlinear behavior of the σ field can be represented somehow in the thermodynamical quantities, by the density dependent constant $\Gamma_\sigma(\rho)$. The same occurs with the ω_0 field, i.e., the strength of the repulsive interaction is also a density dependent quantity, $\Gamma_\omega(\rho)$. Therefore, the DD model can be seen as an effective model in which the nonlinear behavior of the scalar and vector fields are included in the density dependence of the respective couplings. Such a nonlinear behavior of the fields seems to help the model in reaching the experimental values of the critical parameters of Ref. [44]. In the case of the Z271 family, the matching is for all three quantities and for the DD parametrizations, only the T_c experimental value is not reached, with the exception of the DD-ME δ model in which only P_c data matches. A systematic investigation involving a larger number of parametrizations is needed in order to definitely confirm our findings. However, the CRMF models strongly suggest such a phenomenology.

C. Correlations with the incompressibility

As a last investigation concerning the critical parameters, we discuss here whether the correlations found in

Ref. [47] also apply to the CRMF parametrizations. In that work, a strong correlation between T_c , P_c and ρ_c and the incompressibility, K_0 , obtained at zero temperature regime and at the saturation density, was found. For symmetric nuclear matter, the incompressibility of the nonlinear model is given by,

$$K_{\text{NL}} = 9 \left(g_\omega \rho \frac{\partial \omega_0}{\partial \rho} + \frac{k_F^2}{3E_F^*} - g_\sigma \rho \frac{M^*}{E_F^*} \frac{\partial \sigma}{\partial \rho} \right), \quad (14)$$

with

$$\frac{\partial \sigma}{\partial \rho} = \frac{a_1 b_2 + a_2 b_3}{a_1 b_1 - a_3 b_3} \quad \text{and} \quad \frac{\partial \omega_0}{\partial \rho} = \frac{a_2 b_1 + a_3 b_2}{a_1 b_1 - a_3 b_3}, \quad (15)$$

where

$$a_1 = m_\omega^2 + 3Cg_\omega^4 \omega_0^2 + g_\sigma g_\omega^2 \sigma (2\alpha_1 + \alpha'_1 g_\sigma \sigma), \quad (16)$$

$$a_2 = g_\omega, \quad (17)$$

$$a_3 = -2g_\sigma g_\omega^2 \omega_0 (\alpha_1 + \alpha'_1 g_\sigma \sigma), \quad (18)$$

$$b_1 = m_\sigma^2 + 2A\sigma + 3B\sigma^2 - g_\sigma^2 g_\omega^2 \omega_0^2 \alpha'_1 + 3g_\sigma^2 \left(\frac{\rho_s}{M^*} - \frac{\rho}{E_F^*} \right), \quad (19)$$

$$b_2 = \frac{g_\sigma M^*}{E_F^*}, \quad \text{and} \quad b_3 = -a_3. \quad (20)$$

The Fermi momentum is k_F , and $E_F^* = (k_F^2 + M^{*2})^{1/2}$. For the density dependent model, K_{DD} reads

$$K_{\text{DD}} = 9 \left(\rho \frac{\partial \Sigma_R}{\partial \rho} + \frac{2\Gamma_\omega \rho^2}{m_\omega^2} \frac{\partial \Gamma_\omega}{\partial \rho} + \frac{\Gamma_\omega^2 \rho}{m_\omega^2} + \frac{k_F^2}{3E_F^*} + \frac{\rho M^*}{E_F^*} \frac{\partial M^*}{\partial \rho} \right), \quad (21)$$

with

$$\frac{\partial M^*}{\partial \rho} = - \left(\Gamma_\sigma \frac{\partial \sigma}{\partial \rho} + \sigma \frac{\partial \Gamma_\sigma}{\partial \rho} \right) \quad \text{and} \quad (22)$$

$$\frac{\partial \sigma}{\partial \rho} = \frac{\left[\rho_s - 3 \left(\frac{\rho_s}{M^*} - \frac{\rho}{E_F^*} \right) \Gamma_\sigma \sigma \right] \frac{\partial \Gamma_\sigma}{\partial \rho} + \frac{\Gamma_\sigma M^*}{E_F^*}}{m_\sigma^2 + 3 \left(\frac{\rho_s}{M^*} - \frac{\rho}{E_F^*} \right) \Gamma_\sigma^2}, \quad (23)$$

observing the definitions of Eq. (13). In the above expressions, ρ and ρ_s are obtained at $T = 0$ regime by discarding in Eqs. (9)-(10) the antiparticles distribution functions, and by replacing the particle distribution ones by the step function $\theta(k - k_F)$.

In Ref. [47], 128 Boguta-Bodmer parametrizations were analyzed and the critical parameters showed an increasing behavior with K_0 (see Fig. 4). Along that work, it was found that parametrizations with fixed values for the nucleon effective mass present T_c , P_c and ρ_c as clear functions of K_0 (see Fig. 5).

Here, we proceed in the same direction by displaying the critical parameters of the CRMF parametrizations as a function of K_0 in Fig. 4. We separate the points concerning models with different structures, namely, the nonlinear model (circles) and the density dependent one

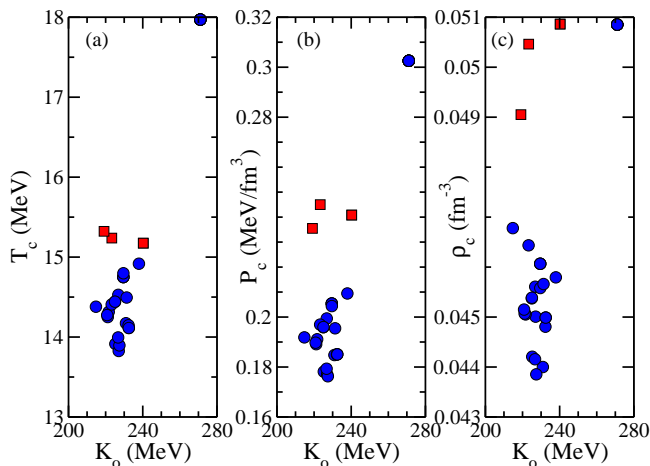


FIG. 4. Critical (a) temperature, (b) pressure, and (c) density of CRMF parametrizations. Circles: nonlinear model. Squares: density dependent model.

(squares). If we consider only the model with more available data, i.e., the nonlinear one, we also verify an indication of T_c , P_c and ρ_c as increasing functions of K_0 , as found in Ref. [47] for the less sophisticated Boguta-Bodmer model. Such general trends are also in line with recent results on classical models for real gases augmented with quantum statistical effects in the description of symmetric nuclear matter, see Ref. [33]. In that work, the author provided the critical temperature of van der Waals, Redlich-Kwong-Soave, Peng-Robinson, and Clausius models. Models with higher values of K_0 also presented higher values of T_c (see Fig. 3).

We have checked that there is no correlation between the critical parameters and other important nuclear matter bulk properties, as the symmetry energy and its slope.

IV. SUMMARY AND CONCLUSIONS

In the present work we have recalculated the critical parameters T_c , P_c and ρ_c , which define the limit-

ing point of the phase transition from a gas to a liquid phase with 34 models, which have shown to satisfy important nuclear matter constraints [6] and reasonably describe stellar matter macroscopic properties [28]. We have divided these models into 6 categories and just two of them (Z271) and (DD) approaches the experimental critical temperature values. By comparing these observations with the neutron star main properties calculated in Ref. [28], we see that only density dependent models seem to behave well both at low and high densities, but this statement requires a more consistent analyses and further experimental and observational data.

We have also verified that the critical parameters present a correlation with the incompressibility, but the same is not true for other important nuclear matter bulk quantities, such as the energy symmetry and its slope.

Finally, we would like to mention that instabilities in neutron- Λ matter are also worth examining. The existence of hypernuclei as bound systems [48] might imply that a similar phase transition in an extended diagram with strangeness as an extra degree of freedom is also present. In Ref. [31], spinodal sections were obtained for matter with couplings fixed so that realistic potentials were reproduced. Hence, investigations about the influence of strangeness on the liquid-gas phase transition and the related critical points are under way.

ACKNOWLEDGMENTS

This work was partially supported by Conselho Nacional de Desenvolvimento Científico e Tecnológico (CNPq), Brazil under grants 300602/2009-0 and 306786/2014-1.

-
- [1] G. Bertsch and P. J. Siemens, Phys. Lett. B **126**, 9 (1983); J. Margueron and P. Chomaz, Phys. Rev. C **67**, 041602 (2003); C. Ducoin, Ph. Chomaz, and F. Gulminelli, Nucl. Phys. A **771**, 68 (2006).
 - [2] H. Müller and B. D. Serot, Phys. Rev. C **52**, 2072 (1995).
 - [3] Ph. Chomaz, C. Colonna, and J. Randrup, Phys. Rep. **389**, 263 (2004).
 - [4] F. Gulminelli, Ad. R. Raduta, and M. Oertel, Phys. Rev. C **86**, 025805 (2012).
 - [5] S.S. Avancini, L. Brito, Ph. Chomaz, D.P. Menezes and C. Providência, Phys. Rev. C **74**, 024317 (2006).
 - [6] M. Dutra, O. Lourenço, S. S. Avancini, B. V. Carlson, A. Delfino, D. P. Menezes, C. Providência, S. Typel, and J. R. Stone, Phys. Rev. C **90**, 055203 (2014).
 - [7] B. K. Agrawal, Phys. Rev. C **81**, 034323 (2010).
 - [8] S. K. Dhiman, R. Kumar, and B. K. Agrawal, Phys. Rev. C **76**, 045801 (2007).
 - [9] B.-J. Cai, L.-W. Chen, Phys. Rev. C **85**, 024302 (2012).
 - [10] B. G. Todd-Rutel and J. Piekarewicz, Phys. Rev. Lett. **95**, 122501 (2005).
 - [11] J. Piekarewicz and S. P. Weppner, Nucl. Phys. A **778**, 10 (2006).
 - [12] R. Kumar, B. K. Agrawal, and S. K. Dhiman, Phys. Rev. C **74**, 034323 (2006).
 - [13] A. Sulaksono and T. Mart, Phys. Rev. C **74**, 045806 (2006).
 - [14] F. J. Fattoyev, C. J. Horowitz, J. Piekarewicz, and G. Shen, Phys. Rev. C **82**, 055803 (2010).

- [15] C. J. Horowitz and J. Piekarewicz, Phys. Rev. C **66**, 055803 (2002).
- [16] T. Klähn, *et al.*, Phys. Rev. C **74**, 035802 (2006).
- [17] S. Typel and H. H. Wolter, Nucl. Phys. **A656**, 331 (1999).
- [18] T. Gaitanos, M. Di Toro, S. Typel, V. Baran, C. Fuchs, V. Greco, and H. H. Wolter, Nucl. Phys. **A732**, 24 (2004).
- [19] X. Roca-Maza, X. Viñas, M. Centelles, P. Ring, and P. Schuck, Phys. Rev. C **84**, 054309 (2011); Phys. Rev. C **93**, 069905(E) (2016).
- [20] J. J. Rusnak and R. J. Furnstahl, Nucl. Phys. A **627**, 495 (1997); D. G. Madland, T. J. Bürvenich, J. A. Maruhn, P.-G. Reinhard, Nucl. Phys. A **741**, 52 (2004).
- [21] O. Lourenço, M. Dutra, A. Delfino, and R. L. P. G. Amaral, Int. Jour. Mod. Phys. E, **16**, 3037 (2007).
- [22] P. W. Zhao, Z. P. Li, J. M. Yao, and J. Meng, Phys. Rev. C **82**, 054319 (2010).
- [23] T. Niksic, D. Vretenar, and P. Ring, Prog. in Part. and Nucl. Phys. **66**, 519 (2011).
- [24] B. A. Nikolaus, T. Hoch, and D. G. Madland, Phys. Rev. C **46**, 1757 (1992).
- [25] A. Sulaksono, T. Bürvenich, J. A. Maruhn, P.-G. Reinhard, and W. Greiner, Ann. Phys. **308**, 354 (2003).
- [26] Y. Tanimura and K. Hagino, Phys. Rev. C **85**, 014306 (2012).
- [27] J. J. Rusnak and R. J. Furnstahl, Nucl. Phys. **A627**, 495 (1997).
- [28] M. Dutra, O. Lourenço, and D. P. Menezes, Phys. Rev. C **93**, 025806 (2016); Erratum: Phys. Rev. C **94**, 049901(E) (2016).
- [29] V. Vovchenko, D. V. Anchishkin, and M. I. Gorenstein, Phys. Rev. C **91**, 064314 (2015).
- [30] V. Vovchenko, D. V. Anchishkin, M. I. Gorenstein, and R. V. Poberezhnyuk, Phys. Rev. C **92**, 054901 (2015).
- [31] J. R. Torres, F. Gulminelli, and D. P. Menezes, Phys. Rev. C **93**, 024306 (2016).
- [32] J. B. Silva, O. Lourenço, A. Delfino, J. S. Sá Martins, M. Dutra, Phys. Lett. B **664** 246, (2008).
- [33] V. Vovchenko, arxiv:1701.06524.
- [34] C. Wu, and Z. Ren, Phys. Rev. C **83**, 044605 (2011).
- [35] G. Mahajan, and S. K. Dhiman, Phys. Rev. C **84**, 045804 (2011).
- [36] A. Fedoseew and H. Lenske, Phys. Rev. C **91**, 034307 (2015).
- [37] R. J. Furnstahl and B. D. Serot, Phys. Rev. C **41**, 262 (1990).
- [38] V. A. Karnaukhov, Phys. At. Nucl. **60**, 1625 (1997).
- [39] J. B. Natowitz, K. Hagel, Y. Ma, M. Murray, L. Qin, R. Wada, and J. Wang, Phys. Rev. Lett. **89**, 212701 (2002).
- [40] V. A. Karnaukhov, *et al.*, Phys. Rev. C **67**, 011601(R) (2003).
- [41] V. A. Karnaukhov, *et al.*, Nucl. Phys. A **734**, 520 (2004).
- [42] V. A. Karnaukhov, *et al.*, Nucl. Phys. A **780**, 91 (2006).
- [43] V. A. Karnaukhov, Phys. At. Nucl. **71**, 2067 (2008).
- [44] J. B. Elliott, P. T. Lake, L. G. Moretto, and L. Phair, Phys. Rev. C **87**, 054622 (2013).
- [45] T. S. Fan *et al.*, Nucl. Phys. A **679**, 121 (2000).
- [46] V. E. Viola *et al.*, Phys. Rep. **434**, 1 (2006); K. Kwiatkowski, Nucl. Instrum. Methods Phys. Res. Sec. A **360**, 571 (1995); T. Lefort, *et al.*, Phys. Rev. Lett. **83**, 4033 (1999); L. Beaulieu, *et al.*, Phys. Rev. Lett. **84**, 5971 (2000); L. Beaulieu, *et al.*, Phys. Rev. C **63**, 031302 (2001).
- [47] O. Lourenço, B. M. Santos, M. Dutra, and A. Delfino, Phys. Rev. C **94**, 045207 (2016).
- [48] D. J. Millener, C. B. Dover, and A. Gal, Phys. Rev. C **38**, 2700 (1988); J. Schaffner-Bielich, M. Hanauske, H. Stocker, and W. Greiner, Phys. Rev. Lett. **89**, 171101 (2002).